

CorrDiff: Adaptive Delay-aware Detector with Temporal Cue Inputs for Real-time Object Detection

Xiang Zhang^{*1}, Chenchen Fu^{*1}, Yufei Cui², Lan Yi¹, Yuyang Sun¹, Weiwei Wu^{**1}, and Xue Liu²

¹School of Computer Science and Engineering, Southeast University, Nanjing, China

²School of Computer Science, McGill University, Montreal, Quebec, Canada

Abstract—Real-time object detection takes an essential part in the decision-making process of numerous real-world applications, including collision avoidance and path planning in autonomous driving systems. This paper presents a novel real-time streaming perception method named CorrDiff, designed to tackle the challenge of delays in real-time detection systems. The main contribution of CorrDiff lies in its adaptive delay-aware detector, which is able to utilize runtime-estimated temporal cues to predict objects' locations for multiple future frames, and selectively produce predictions that matches real-world time, effectively compensating for any communication and computational delays.

The proposed model outperforms current state-of-the-art methods by leveraging motion estimation and feature enhancement, both for 1) single-frame detection for the current frame or the next frame, in terms of the metric mAP, and 2) the prediction for (multiple) future frame(s), in terms of the metric sAP (The sAP metric is to evaluate object detection algorithms in streaming scenarios, factoring in both latency and accuracy). It demonstrates robust performance across a range of devices, from powerful Tesla V100 to modest RTX 2080Ti, achieving the highest level of perceptual accuracy on all platforms. Unlike most state-of-the-art methods that struggle to complete computation within a single frame on less powerful devices, CorrDiff meets the stringent real-time processing requirements on all kinds of devices. The experimental results emphasize the system's adaptability and its potential to significantly improve the safety and reliability for many real-world systems, such as autonomous driving. Our code is completely open-sourced and is available at <https://anonymous.4open.science/r/CorrDiff>.

Index Terms—Real-time systems, Object recognition, Streaming perception, Delay adaptation, Temporal reasoning

I. INTRODUCTION

IN the rapidly evolving field of autonomous driving, the capability to detect and track objects in real-time is paramount for ensuring safety and efficiency. The pursuit of this capability has led to a surge in research with two critical objectives: enhancing detection accuracy [17], [18] and minimizing model latency [4], [19]. Apparently, the simultaneous consideration of both objectives is vital for applications such as self-driving cars, where instant detection is necessary for immediate decision-making. Real-time object detection, also known as streaming perception, has thus gained attraction in recent years due to its role in comprehending the dynamic motion of the surrounding environment, and targets to do accurate detections with minimal delays, meeting the demands of real-time processing.

To meet real-time requirements, initial approaches attempted to enhance the speed of non-real-time detectors to achieve a

higher frame rate of detection. However, as [15] highlighted, even with accelerated detectors, there are inherent delays in real-world applications. By the time a detector processes a frame, the environment has changed. This results in the temporal gap between the input of a frame and the output of a prediction, which can be fatal in scenarios where every millisecond counts, like autonomous driving. As shown in Figure 1, the detection is accurate in an ideal environment, where the detection process finishes instantly without any delays. However, a real-world environment would incur the non-negligible communication-computational delay in the detection process, causing a displacement between detection results (based on the input scenario) and the actual objects.

In response to this critical issue, recent studies [10], [12], [14], [15], [25] have augmented detectors with predictive capabilities, by training models to anticipate future objects' positions. *However, these methods typically forecast object locations at a fixed interval (typically a single frame ahead), and expect the data communication together with the computation process to complete within the single frame interval [25].* For instance, a video stream with a frame rate of 30 would require the detection operation to complete within 1/30 of a second. So detectors must process the frame within strict time constraints, which means that most competent models strictly require low communication overhead and fast GPU processing [10], [14], [25] even under diverse situations.

In this work, we observed and focused on an often-overlooked but significant issue: **in the real world, the communication-computational delays vary significantly over time as communication bandwidth and workloads fluctuate and thus cannot be guaranteed to complete the whole detection process within a single frame.** As illustrated in Figure 2.(a), the same detector (the SOTA method DAMO-StreamNet [10]) faces widely different delays in one-frame inference across different devices. And even applied on the same device, the same detector experiences delays ranging from 27ms to 58ms depending on the system's workload as in Figure 2.(b). Delay fluctuations are also observed under different bandwidth limitations as shown in Figure 2.(c). This variability suggests that models may struggle to meet consistent real-time constraints during peak workloads or under low bandwidth, which could lead to critical failures in accurate real-time detection.

To address this critical issue, this work introduces CorrDiff, a novel method that leverages temporal cues to integrate runtime information into the detection model. CorrDiff takes

* Equal contribution

** Corresponding author

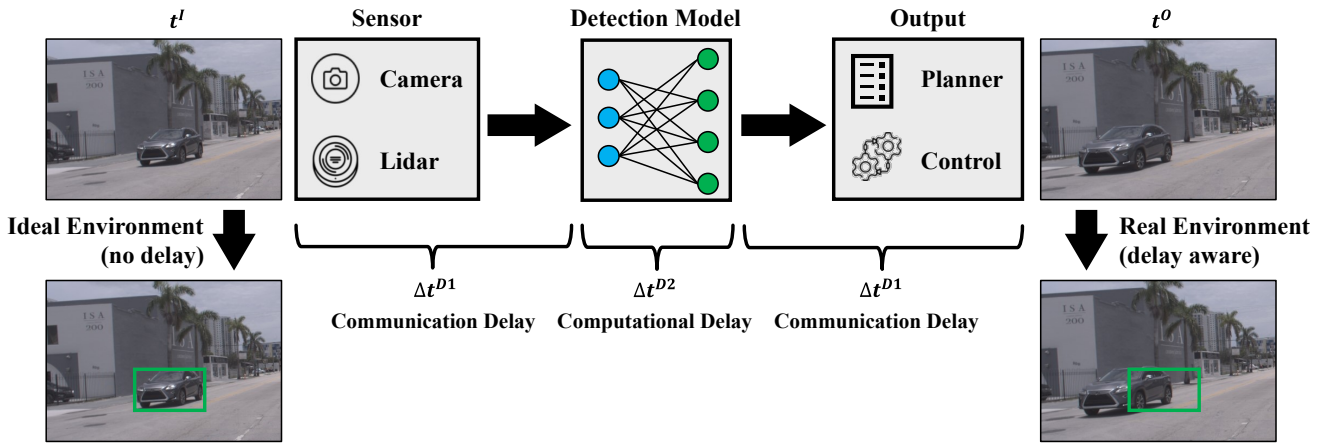


Fig. 1. Demonstration of object displacement error in real world systems with potential communication-computational delays.

multiple past frames as input, producing predictions for multiple future frames simultaneously, while allowing for flexible output selection to adapt to delay fluctuations. The framework is specifically designed to tackle the challenges of real-time object detection under varying and dynamic delay conditions. The primary contributions of this work are summarized as follows.

- This work enables adaptive delay-aware streaming perception by integrating runtime information directly within detection models, concurrently predicting multiple frames and selectively produce the most appropriate output aligned with the real-world present time.
- Even in the realm of single-frame real-time detection, the proposed approach still outperforms all the existing state-of-the-art (SOTA) techniques.
- The proposed model demonstrates robust performance across a spectrum of devices, with GPUs that ranging from the high-performance Tesla V100 to the modest RTX 2080Ti. It achieves the highest level of perceptual accuracy on all platforms, whereas most SOTA methods struggle to complete computation within a single frame when applied on less powerful devices, thereby failing to meet the stringent real-time processing requirement.

For the rest of the paper, we will discuss relevant literature and potential gaps in Section II, the motivation of our approach in Section III, the methodology in Section IV and the performance comparisons in Section V.

II. RELATED WORK

Image Object Detection: The evolution of deep learning has dramatically influenced the realm of object detection, with CNNs outpacing traditional methods. Image object detection methods are primarily divided into two-stage and one-stage methods. Two-stage methods are exemplified by R-CNN [8], which boosted accuracy by integrating region proposals with CNN features. Advancements in the two-stage approaches, seen in Fast R-CNN [7] and Faster R-CNN [20], streamlined the process by merging region proposal networks with CNN architecture. Nevertheless, these techniques still experience delays due to proposal refinement. In contrast, one-stage methods such as SSD [16] and YOLO [19], further removed

the dependency on region proposals to reduce latency. They offered a balance of speed and precision for real-time tasks but lacked the temporal context necessary for streaming detection, as they focused solely on the current frame.

Video Object Detection: Video object detection (VOD) aims to detect objects on video data instead of static images. While early approaches processed each frame independently, they obviously failed to utilize video characteristics. Recent deep learning methods seek to make use of temporal-spatial relationship in the following means. Flow-based methods [22], [26]–[28] estimated optical flows to enhance the features of non-key frames. Tracking-based methods [3] aimed to build object connections by learning feature similarities across frames. Attention-based methods [2], [9], [21], [23] applied attention mechanisms to establish temporal context relationships on long-duration videos. While these methods interpreted temporal information in various approaches, they generally focused on the offline setting, where detection delay is often overlooked. Contrastingly, this work takes both delay and temporal-spatial context into consideration, ensuring high accuracy with real-time performance.

Streaming Perception: Streaming perception aims to tackle the drift in real-time detection results caused by system latency. This drift is compensated by predicting entity locations after a certain number of frames using temporal information from historical results [15]. The sAP metric was introduced to evaluate object detection algorithms in streaming scenarios, factoring in both latency and accuracy. Chanakya [5] attempted to improve sAP performance by learning a policy to alter input resolution and model size, efficiently balancing latency and accuracy. However, Chanakya did not base its method on a temporal-predictive detector. Subsequent researches thus introduced several models aimed at forecasting object locations. For example, StreamYOLO [25] used a dual-flow perception module for next-frame prediction, combining both previous and current frames' features. Dade [12] and MTD [11] introduced mechanisms to dynamically select features from past or future timestamps, taking the runtime delay of the algorithm into consideration. DAMO-StreamNet [10] and Longshortnet [14] used dual-path architectures to capture long-term motion and calibrate with short-term semantics. They

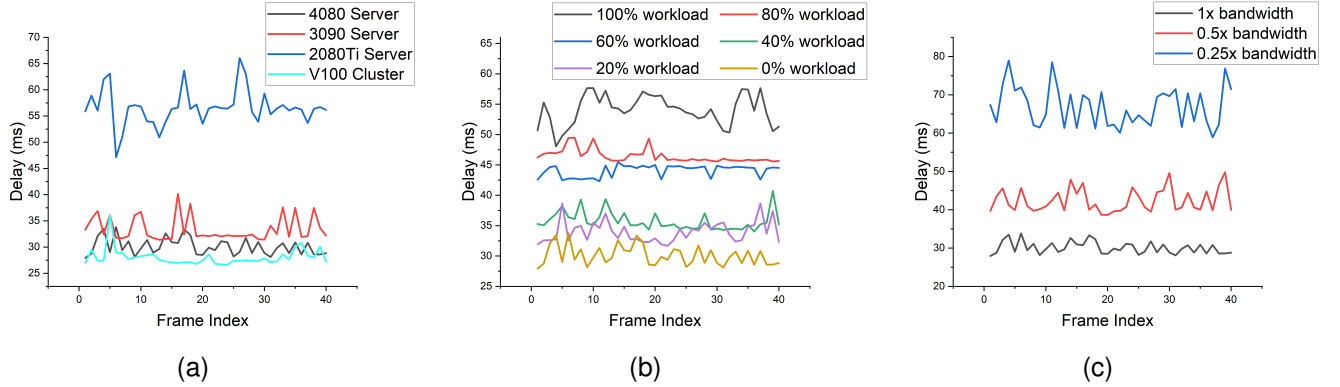


Fig. 2. One-frame inference delay of the DAMO-StreamNet [10] in different scenarios: (a) deploying on different devices. (b) deploying on a server with RTX 4080 but with various workloads (simulated by using a similar approach to GPU contention generation in [24]). (c) deploying on a server with RTX 4080 but with different bandwidths.

extended dynamic flow path from 1 past frame to 3 past frames, successfully capturing the long-term motion of moving objects, and thus achieved the state-of-the-art performance in streaming perception. **These existing studies, however, only forecast objects' locations in the next frame, expecting the detector to finish computations within one frame.** Such approaches are infeasible on real-world devices, where potential communication-computational delays vary significantly and the whole detection process cannot be guaranteed within a single frame. Our proposed method is delay-aware and handles situations with high and dynamic lags. With the capability of using temporal cues inside detection model, our method is able to accommodate various communication-computational delays.

III. MOTIVATION AND PROBLEM FORMULATION

Though communication-computational delays in real-time object detection have been studied in some research, the existing studies only produced a fixed-interval output (predicting the fixed one frame ahead [10], [25]), and thus failed to adapt to the dynamic nature of delays. In the following, we will show the observation of the real-world problems, which motivates this work.

A. Observation and Motivation

The existing studies in streaming perception [10], [14], [25], which focused on fixed frame prediction, also have noticed that various object displacement may be involved by different moving velocity of vehicles, which can significantly affect the real-time detection. For instance, if the detector is only trained at a fixed frame rate (e.g., 60 frames per second (FPS)), it can only be equipped to simulate vehicles moving at a corresponding constant speed (e.g., 30km/h). As depicted in Figure 3.(a) and Figure 3.(c), when a vehicle's speed increases to 60km/h, the detector (trained at the fixed frame rate to simulate 30km/h) fails to accurately detect it.

To address the above mentioned issue, training schemes with speed variation were applied in these work [10], [14], [25], and thus the trained model is capable to do detection on different speeds. However, they need to fix the speed before applying

the model, i.e., at each frame i , determine that whether they do the detection for frame $i + 1$ to simulate slow vehicle velocity or do detection for frame $i + 3$ to simulate fast vehicle velocity. These approaches thus are inherently restrictive because they did not allow dynamic velocity of vehicles in runtime.

In fact, we observed that dynamic and significant delays can be involved in one-frame detection for the detection model like DAMO-StreamNet [10], because of various issues such as dynamic workloads or different bandwidth, as shown in Figure 2.(b) and Figure 2.(c). Other dynamic workloads could occupy GPU memory and utilization, affecting the computational delay of the model. Bandwidth variations could limit the speed of data and increase the communication delay.

As a result, even the vehicle velocity remains the same (30km/h), as shown in Figure 3.(a) and 3.(b), different communication-computational delay will lead to inaccurate detection as it takes different duration to generate the output. It can be noted that various velocities and dynamic delays introduce a similar element of randomness during the detection process, complicating the prediction task.

To address these challenges, we introduce CorrDiff, a novel approach that captures the inherent randomness in both vehicle velocity and communication-computational delays. Our solution is designed to provide real-time detection via dynamic prediction generation for multiple future frames utilizing temporal cues, adapting to various delays and object displacements. Specifically, CorrDiff is tailored to accommodate diverse runtime scenarios, thereby enhancing the safety and reliability of streaming perception systems in various operational contexts.

B. Problem Formation

Given a real-time monocular video sequence $\{I_i\} \in \mathbb{R}^{length \times 3 \times h \times w}$, the proposed method aims to generate the bounding box predictions $\{\hat{O}_i\} \in \mathbb{R}^{length \times Objects \times 5}$ for each timestamp. During the streaming perception evaluation process, each frame is emitted at timestamp $t_i^I = \frac{i}{k}$, where k is the frame rate (30 frames per second (FPS), typically). As described in Figure 1, while the detector is inferring the frames, potential delays will happen, which leads to a misaligned timestamp of the outputs $\{t_i^O\}$ compared to the inputs $\{t_i^I\}$. Generally, the

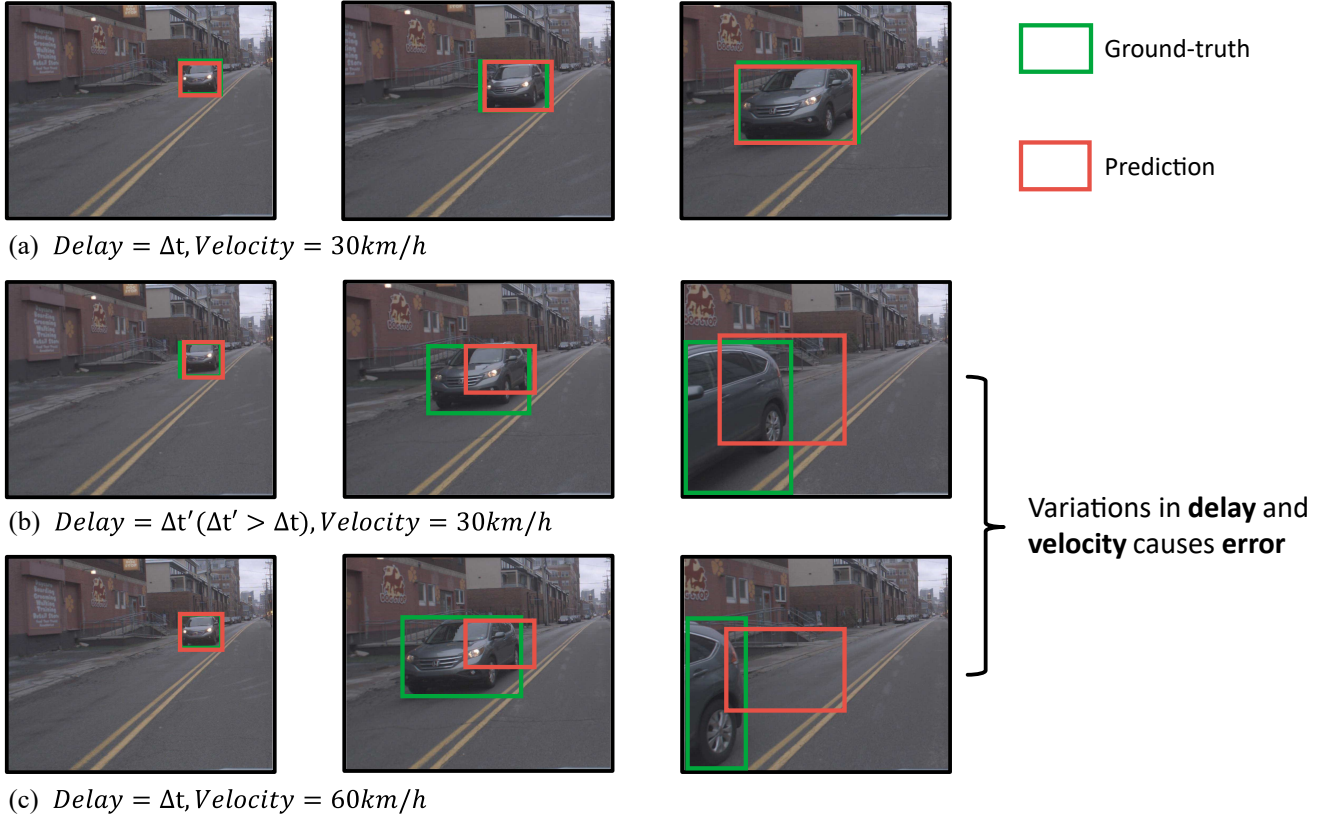


Fig. 3. Motivation example: when a streaming detector is trained with fixed communication-computational delay (e.g. Δt) and fixed object velocities (e.g. $30km/h$), the inference can be accurate when (a) both delay and velocity remain the same as in training. But the detection accuracy will significantly decrease when either (b) the communication-computational delay varies (e.g. from Δt to $\Delta t'$) or (c) the vehicle velocity changes (e.g. from $30km/h$ to $60km/h$).

delays compose of communication delay Δt^{D1} , computational delay Δt^{D2} and optional start-up delay Δt^{D3} (delay caused by not finishing the process of the previous frames before the current frame). Denote the sum of these delays as Δt , and thus we have

$$t_i^O = t_i^I + \Delta t_i = t_i^I + \Delta t_i^{D1} + \Delta t_i^{D2} + \Delta t_i^{D3}. \quad (1)$$

The existing studies either assume $\Delta t_i = 0$ (the non-real-time detectors such as Fast-RCNN [7]), or assume it costs fixed number of frames, e.g. 1 frame ([10], [14], [25]). For the latter case, they did prediction at t_{i-1}^I to obtain the prediction of current frame \hat{O}_i at t_{i-1}^O , forcing the detection process to complete within one frame ($t_{i-1}^O < t_i^I$).

An interesting and important observation from realistic system is that the delay is non-negligible and varies significantly. This requires the algorithm to have the ability to forecast the objects' locations across multiple future frames, as various delays may occur. It should manage to compensate the object displacement error caused by communication delay Δt^{D1} , computational delay Δt^{D2} , and potential start-up delay Δt^{D3} . The algorithm's capabilities are formally defined as follows:

- For longer delays spanning more than a single frame, the detector needs to be capable of accurately predicting farther future across multiple frames. Denote the current frame as I_i , given the past frames I_{i-1}, I_{i-2}, \dots , we generate a series of prediction $\hat{O}_{i+1}, \hat{O}_{i+2}, \dots$.

- With dynamic delays, the detector should be able to adaptively output the correct detection \hat{O}_j out of all the predictions, that aligned to the real world timing t_i^O . \hat{O}_j will be evaluated by comparing to ground-truth O_j .
- Moreover, under realistic conditions, communication errors may render a frame I_i unavailable. The detector should still be able to generate predictions under such circumstance.

Building on these requirements, we propose CorrDiff, a novel method that not only meets the aforementioned capabilities but also satisfies stringent real-time processing demands across various devices in realistic scenarios.

IV. METHODOLOGY

In order to fill the research gap presented in current literature, we proposed CorrDiff, a detection system composes of a detection model named CDdetector and a scheduling algorithm named CDScheduler, to accommodate runtime delays and incorporate temporal cues inside the model. The detailed architecture is clarified in the following paragraphs.

A. Overall Design of CorrDiff

The general architecture of the proposed method CorrDiff is shown in Figure 4. As a solution for real-time streaming detection, CorrDiff consists of 2 main modules, a CNN-based detection model CDdetector and a scheduling algorithm CDScheduler. CDdetector is capable of utilizing runtime temporal

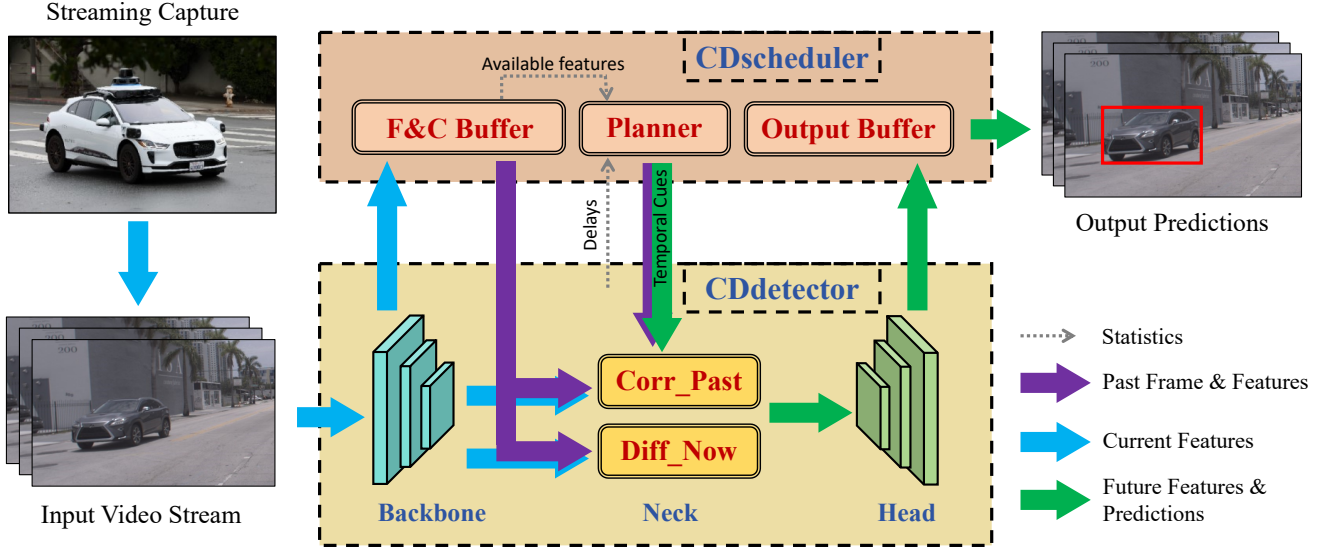


Fig. 4. Overall architecture of CorrDiff. CorrDiff composes of a detection model CDdetector and a scheduling algorithm CDScheduler. CDdetector utilizes the Corr_Past module and the Diff_Now module, combining past and current features to produce future predictions. CDScheduler provides support by gathering runtime statistics to generate Temporal Cues, which is proceeded by CDdetector, making it adaptively delay-aware. The scheduler also uses 3 buffers: Historical Feature Buffer to reuse previously computed frame features, Corr_Past Buffer to reuse correlation results and Output Buffer to store the freshest predictions and dispatch detection results at the corresponding timestamp. F&C Buffer is the abbreviation for Historical Feature Buffer and Corr_Past Buffer.

information, processing multiple past frames and generating predictions for multiple future frames. Meanwhile, CDScheduler assists CDdetector to adapt to various runtime conditions by collecting runtime statistics and providing CDdetector with temporal cues to guide its execution.

In the following, for the detection model CDdetector, we firstly introduce 2 submodules named Corr_Past and Diff_Now to capture the temporal movement of observed objects. These 2 blocks utilizes past and future temporal cues, to fuse past frames' features and to predict the features for future frames. The past and future temporal cues denoted as C^P and C^F respectively, which indicates the indices of past frames and desired future predictions. At inference time, the model is paired with the scheduling algorithm CDScheduler to generate C^P and C^F , determining the choice of input frames $\{I_j\}, j \in C^P$ and desired output predictions $\{\hat{O}_j\}, j \in C^F$. Next, for CDScheduler, we propose a method to compute temporal cues C^P and C^F from collected or estimated runtime statistics $\Delta \hat{t}^{D1}, \Delta \hat{t}^{D2}$ and Δt^{D3} . Apart from using runtime information, CDScheduler also uses Historical Feature Buffer and Corr_Diff Buffer (together abbreviated as F&C Buffer in Figure 4) to hold previously generated image features and correlation features in a streaming fashion, in order to avoid recomputation and reduce Δt^{D2} . While the model outputs detection results for multiple future frames, the output predictions are stored inside Output Buffer and dispatched at its corresponding timestamp. In this buffer, newer or fresher predictions can update elder ones if they have not been dispatched.

B. CDdetector: The Detection Model

In the proposed method, we separate the design of CDdetector into 3 submodules: a DRFPN backbone for feature extraction, a CD neck for temporal feature fusing and forecasting, and a TAL head for predicting and decoding bounding

boxes. Our work focuses on developing a neck module that utilizes temporal information to fuse multiple past frames' features, guiding the prediction of future objects' locations. We use the same backbone (DRFPN) and head (TAL) as in [10], [25].

At inference time, the model is given the current frame I_i , buffered previous frames' features $\{F_j\}, j \in C^P \setminus \{i\}$ and the temporal cues C^P, C^F . CDdetector is required to generate future frames' predictions $\{\hat{O}_j\}, j \in C^F$. Firstly, the features of the current frame is extracted by the backbone module $\mathbf{W}^B(\cdot)$ and then concatenated to the buffered features \mathcal{F}^P in a chronological order, producing past frames' features $\mathcal{F}^P = \{F_j\}, j \in C^P$. Secondly, \mathcal{F}^P is fed into the CD neck, which has 2 branches: Corr_Past (Temporal Correlation, denoted as $\mathbf{W}^C(\cdot)$) and Diff_Now (Temporal Difference, denoted as $\mathbf{W}^D(\cdot)$). Corr_Past captures the potential movements of temporal features, while Diff_Now enhances the quality of the current feature. These submodules merge past and current features to produce future frames' features $\mathcal{F}^F = \{F_j\}, j \in C^F$. Finally, the head module $\mathbf{W}^H(\cdot)$ process the future frames' features \mathcal{F}^F in the same way as in ordinary object detection models, generating the estimated bounding boxes for future objects $\hat{O} = \{\hat{O}_j\}, j \in C^F$. Note that when the current frame I_i is unavailable, detection process will start from the CD neck using previously stored buffers \mathcal{F}^P and updated temporal cues C^P, C^F . The CDdetector can be described as

$$\mathcal{F}^P = \text{Concat}(\mathbf{W}^B(I_i), \{F_j\}) \quad (2a)$$

$$\mathcal{F}^F = \text{Dup}(F_i) + \mathbf{W}^C(\mathcal{F}^P, C^P, C^F) + \mathbf{W}^D(\mathcal{F}^P) \quad (2b)$$

$$\hat{O} = \mathbf{W}^H(\mathcal{F}^F), \quad (2c)$$

where i denotes the index of current frame, $j \in C^F$ denotes the index of past frames. Concat denotes tensor concatenation and

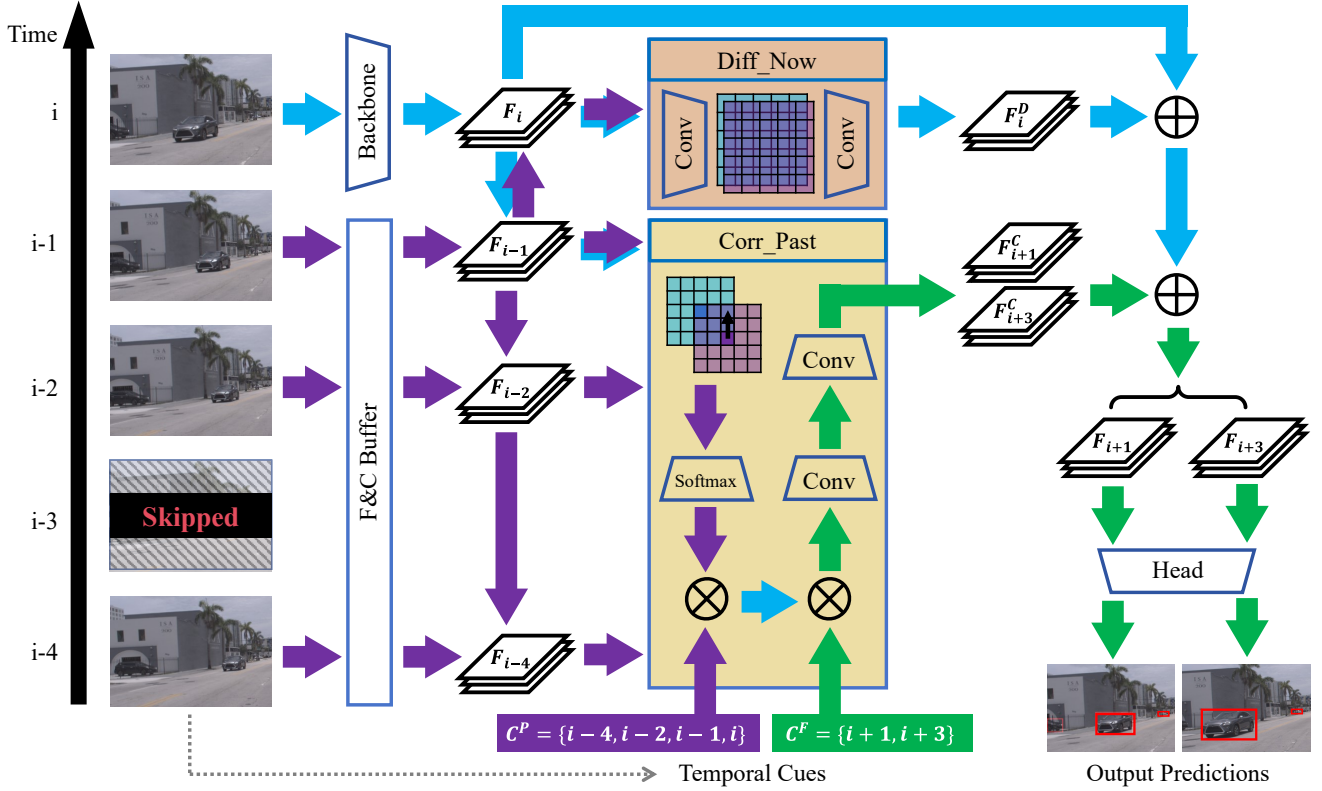


Fig. 5. Detailed architecture of the detection model CDdetector. The example illustrates the situation that $i - 3$ frame is skipped due to communication or computational delay. The detector is required to generate predictions for frame at $i + 1$, $i + 3$, given the image at i and buffered features at $i - 1$, $i - 2$, $i - 4$.

Dup denotes feature duplication along the temporal dimension. The whole architecture of CDdetector is shown in Figure 5.

Corr_Past: The Corr_Past module aims to capture the temporal dynamics of the past frame features. Inspired by optical flow models such as FastFlowNet [13], we utilize a spatial correlation sampler to measure the similarity between adjacent feature pixels across the temporal dimension. To ensure numerical stability, normalization is applied to prevent floating-point overflow. For each past feature $F_j, j \in C^P \setminus \{i\}$, we compute its correlation with the feature of the next available past frame, $F_{j'}$. For each point x in $F_j(x)$, we calculate its similarity in a local neighborhood of $F_j(x)$, defined as $x + r_1$, where $r_1 \in \mathcal{R}_1 = [-R_1, R_1] \times [-R_1, R_1]$. The similarity of 2 points is then determined by computing the dot product of their feature vectors and summing over a local region $\mathcal{R}_2 = [-R_2, R_2] \times [-R_2, R_2]$. Mathematically, the correlation of two frame features can be expressed as

$$\begin{aligned} F_j^{C1}(x) &= \text{Concat}(\text{Similarity}(F_j(x), F_{j'}(x + r_1))) \\ &= \text{Concat}(\sum_{r_1 \in \mathcal{R}_1} \sum_{r_2 \in \mathcal{R}_2} F_j(x + r_1) \cdot F_{j'}(x + r_1 + r_2)), \end{aligned} \quad (3)$$

where Concat denotes tensor concatenation along \mathcal{R}_1 and Similarity denotes similarity between 2 points. The output of the correlation operation is denoted as $\{F_j^{C1}, j \in C^P \setminus \{i\}\}$.

To get an indicator of the overall movement of the current frame, we use weighted sum to fuse every F_j^{C1} . The weights

are calculated by the softmax of C^P , the past temporal cue. We also multiply it with the future temporal cue C^F to get the movement of every future frame. The resulting correlation $\{F_j^{C2}, j \in C^F\}$ is then concatenated with F_i along the channel dimension, followed by 2 convolution operations to cast it back to its original number of channels. In practice, only the deepest feature from the feature pyramid is used. The correlation is up-sampled along spatial dimensions to match other feature in the feature pyramid. This method can capture movement in deep features with rich semantical context, lowering computation costs at the same time. The resulting feature is regarded as the correlation feature and denoted as $\{F_j^C, j \in C^F\}$.

Diff_Now: Beside used to capture movement, past features $\{F_j, j \in C^P\}$ can also be used to enhance the features of the current frame F_i . Adjacent frame's features can be used to clarify certain ambiguous areas in current frame's features. Diff_Now firstly choose the most neighboring feature $F_{max(j)}$ and both features pass a convolution block. The current feature is then subtracted by the neighboring feature, in order to distinguish the difference between these features. The resulting feature is regarded as the difference feature and denoted as F_i^D . The process of Diff_Now is described as

$$F_i^D = \text{Conv}_2(\text{Conv}_1(F_i) - \text{Conv}_1(F_{max(j)})), \quad (4)$$

where Conv_1 and Conv_2 denote convolution blocks.

Combination: While the correlation and difference features are computed, a residual connection from the current frame's feature is still needed. We argue that the current frame's feature

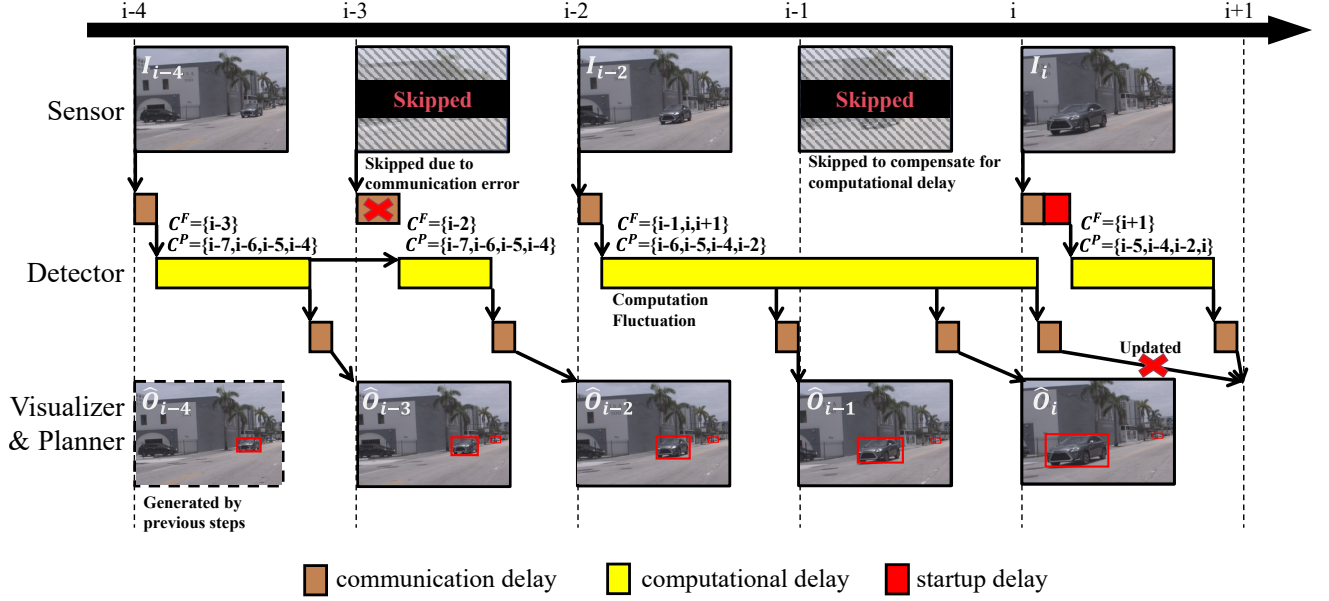


Fig. 6. Demonstration of the scheduling algorithm CDScheduler. C^P , C^F are temporal cues that determine the utilized past features and target future predictions of CDdetector. When communication errors or delays occur, the scheduler adjusts the temporal cues to let CDdetector skip unavailable frames and forecasts further into the future. It can be noted that the proposed method can guarantee accurate prediction output at each timestamp to satisfy real-time requirements.

is a reasonable initial guess of future frames' features. To this end, we firstly add F_i with F_i^D , then duplicate it among the temporal dimension. The duplicated features are then added with $\{F_j^C\}$ to produce $\{F_j\}$, $j \in C^F$, as the input to the head module. Finally, the CD neck can be mathematically represented as

$$\{F_j\} = \text{Dup}(F_i + F_i^D) + \{F_j^C\}, \quad (5)$$

where i denotes the index of current frame and $j \in C^F$ denote future indices.

C. CDScheduler: The Scheduling Algorithm

CDScheduler is responsible for generating temporal cues and arrange model execution, consisting of a Planner and three buffers. The Planner is the core of the algorithm. It collects and estimates runtime statistics to produce the temporal cues. The Planner also skips model execution when there is little time before the arrival of the following frame. The three buffers are: Historical Feature Buffer, Corr_Past Buffer and Output Buffer. The first two buffers accelerate model execution by avoiding recomputation, while the Output Buffer dispatches multi-frame detection results to align with the real world timing and updates elder predictions with newer ones.

Planner: The main function of the Planner is to generate an appropriate C^P and C^F so that the detection model's performance is maximized under Streaming Perception settings. During streaming inference, the communication delay, as well as the previous computation time of CDdetector's backbone, neck and head module, are firstly recorded as $\{\Delta t_j^{D1}, \Delta t_j^{D2B}, \Delta t_j^{D2N}, \Delta t_j^{D2H}\}$, $j < i$. As a reasonable guess, we estimate these delays in the current loop $\{\Delta \hat{t}_i^{D1}, \Delta \hat{t}_i^{D2B}, \Delta \hat{t}_i^{D2N}, \Delta \hat{t}_i^{D2H}\}$ with exponential moving

average (EMA) of Δt_j with a decay of 0.5. Additionally, the start-up delay of the current loop can be directly measured as Δt_i^{D3} . Therefore, the total estimated delay $\Delta \hat{t}_i$ can be denoted as:

$$\Delta \hat{t}_i = \begin{cases} \Delta \hat{t}_i^{D1} + \Delta \hat{t}_i^{D2B} + \Delta \hat{t}_i^{D2N} + \Delta \hat{t}_i^{D2H} + \Delta \hat{t}_i^{D3}, & \text{the current frame } I_i \text{ is available} \\ \sum_{j \in S} \Delta t_j + \Delta \hat{t}_i^{D1} + \Delta \hat{t}_i^{D2N} + \Delta \hat{t}_i^{D2H} + \Delta \hat{t}_i^{D3}, & \text{the current frame } I_i \text{ is unavailable} \end{cases} \quad (6)$$

where S denotes the indices of other skipped adjacent frames. When the current frame is unavailable, we reuse previously computed past features so that the computational delay of the backbone $\Delta \hat{t}_i^{D2B}$ is not included in $\Delta \hat{t}_i$. To fully utilize past buffers, we select at most m^P latest available buffers' indices as C^P . Planner also limits the future predictions by producing at most m^F predictions, indexed as C^F . The future indices C^F approximate estimated output time $t_i^t + \Delta \hat{t}_i$. Finally, both C^P and C^F are clipped within the range of $[i-30, i+30]$ to keep temporal perception in reasonable range. The values are assigned empirically. This solution manages to maintain the balance between model latency and forecasting accuracy with respect to high and fluctuating delays. The demonstration of runtime statistics collection and temporal cue calculation are shown in Figure 6. The figure depicts the situation where frame skips occurred due to communication error and computation delay. The Planner correctly produces the temporal cues to guide CDdetector into predicting frames that cover all timestamps.

Historical Feature Buffer: Though the features of past frames $\{F_j\}$, $j \in C^P$ can be directly acquired by backbone inference $\{\mathbf{W}^B(I_j)\}$, such method is not applicable in streaming



Fig. 7. Demonstration of Non-real-time methods and CorrDiff on the Argoverse-HD dataset under streaming perception settings. Non-real-time methods (a) exhibits large object displacement error for its long communication and computation delay. CorrDiff (b) manages to produce up-to-date results for its low inference time and its ability to adapt to different delays and objects velocities.

evaluations, where the computation load clearly affects the final performance. Therefore, we cache historical frame’s feature to avoid recomputation. We also set a limit to the length of the buffer and choose to discard the earliest buffered features after the buffer is full. Since early frames have a negligible influence on the current frame, the limitation ease the computation burden of the DRFPN backbone module, which has very large amount of parameters compared to other modules.

Corr_Past Buffer: During the computation of Corr_Past, we can observe that the correlation feature between previous frames can also be saved to avoid recomputation. Specifically, we can save the correlation features of the past frames $\{C_j\}$. Since these features are irrelevant to the current feature, the following computations can reuse it.

Output Buffer: Although multiple future object predictions $\{\hat{O}_j\}, j \in C^F$ are produced by CorrDiff, they should not be emitted directly in sequential order. Because it may produce outdated result when $\Delta\hat{t}_i$ is underestimated. Therefore, we apply another buffer to the output of CorrDiff. At every timestamp, most temporally adjacent predictions in the buffer are dispatched, in order to effectively utilize all the predictions at appropriate timestamps. Furthermore, a newer prediction for index j can update the older one if the older one still resides in the buffer.

D. Training and Inference

We mostly replicate the training scheme used by baseline methods [10], [14], with the exception of Asymmetric Knowledge Distillation proposed by [10], since we believe this contribution is orthogonal with our work.

Mixed Speed Training: To enhance model’s delay-awareness, we also employ mixed speed training to extend

the temporal perception range of CorrDiff. The model will be ineffective under other delays and velocities if only a fixed choice of temporal cues C^P and C^F is used for training. Therefore, we adopt mixed speed training scheme that samples C^P from $[-16, 0]$ and C^F from $[1, 16]$. The loss for each predicted future object is given equal weights.

V. EXPERIMENT

In this section, the implementations of both our method and evaluation metrics are elaborated. We also report the performances and ablation results of our method.

A. Implementation Details

Dataset: We trained and tested CorrDiff on Argoverse-HD, an urban driving dataset composed of the front camera video sequence and bounding-box annotations for common road objects (e.g. cars, pedestrians, traffic lights). This dataset contains high-frequency annotation of 30 FPS that simulates real-world environment, which is suitable for streaming evaluation. We believe other datasets (e.g. nuScenes, Waymo) are not suitable for streaming evaluation as they are annotated at a lower frequency. We follow the train and validation split as in [10].

Model: The base backbone of our proposed model is pretrained on the COCO dataset, which is consistent with the approach of [10]. Other parameters are initialized with Lecun weight initialization. The model is then fine-tuned on the Argoverse-HD dataset for 8 epochs using a single Nvidia GeForce RTX 4080 GPU with a batch size of 4 and half-resolution input (600×960). To ensure a fair comparison with other methods, we provide 3 configurations of CorrDiff: CorrDiff-S (small), CorrDiff-M (medium) and CorrDiff-L

TABLE I

MAIN RESULT OF SAP COMPARISON WITH REAL-TIME AND NON REAL-TIME SOTA DETECTORS ON THE ARGOVERSE-HD DATASET. BEST SAP SCORES ARE INDICATED IN BOLD.

Methods	sAP	sAP_{50}	sAP_{75}	sAP_S	sAP_M	sAP_L
Non Real-time Methods						
Streamer (S=900) [15]	18.2	35.3	16.8	4.7	14.4	34.6
Streamer (S=600) [15]	20.4	35.6	20.8	3.6	18.0	47.2
Streamer + AdaS [1], [6]	13.8	23.4	14.2	0.2	9.0	39.9
Adaptive Streamer [6]	21.3	37.3	21.1	4.4	18.7	47.1
YOLOX-S [4]	25.8	47.0	24.3	8.8	25.7	44.5
YOLOX-M [4]	29.4	51.6	28.1	10.3	29.9	50.4
YOLOX-L [4]	32.5	55.9	31.2	12.0	31.3	57.1
Real-time Methods						
StreamYOLO-S [25]	28.8	50.3	27.6	9.7	30.7	53.1
StreamYOLO-M [25]	32.9	54.0	32.5	12.4	34.8	58.1
StreamYOLO-L [25]	36.1	57.6	35.6	13.8	37.1	63.3
DADE-L [12]	36.7	63.9	36.9	14.6	57.9	37.3
LongShortNet-S [14]	29.8	50.4	29.5	11.0	30.6	52.8
LongShortNet-M [14]	34.1	54.8	34.6	13.3	35.3	58.1
LongShortNet-L [14]	37.1	57.8	37.7	15.2	37.3	63.8
DAMO-StreamNet-S [10]	31.8	52.3	31.0	11.4	32.9	58.7
DAMO-StreamNet-M [10]	35.7	56.7	35.9	14.5	36.3	63.3
DAMO-StreamNet-L [10]	37.8	59.1	38.6	16.1	39.0	64.6
CorrDiff-S(Ours)	32.1	53.1	32.0	11.4	33.5	61.0
CorrDiff-M(Ours)	36.0	57.5	36.2	14.6	36.9	64.6
CorrDiff-L(Ours)	38.1	59.4	39.0	16.6	39.5	65.7

TABLE II

DELAY ADAPTATION METRIC COMPARISON WITH DIFFERENT REAL-WORLD DEVICES. * MEANS THE MODEL IS TRAINED USING MIXED SPEED TRAINING TECHNIQUE. BEST SAP SCORES ARE INDICATED IN BOLD.

Devices	Methods	sAP^2	sAP^4	sAP^8	sAP^{16}
v100 cluster	LongShortNet-S	25.5	21.6	16.7	11.0
	DAMO-StreamNet-S	25.0	19.9	14.2	9.4
	CorrDiff-S*(Ours)	26.1	22.2	16.8	12.0
4080 server	LongShortNet-S	24.5	20.3	14.8	9.8
	DAMO-StreamNet-S	23.9	18.5	12.7	8.8
	CorrDiff-S*(Ours)	25.0	20.8	15.6	11.0
3090 server	LongShortNet-S	24.0	20.0	14.4	9.5
	DAMO-StreamNet-S	23.7	18.2	12.6	8.8
	CorrDiff-S*(Ours)	24.7	20.5	15.2	10.6
2080Ti server	LongShortNet-S	23.0	18.0	12.7	8.6
	DAMO-StreamNet-S	21.9	16.4	11.3	8.0
	CorrDiff-S*(Ours)	23.3	18.7	13.2	9.4

TABLE III

ACCELERATION ADAPTATION METRIC COMPARISON WITH DIFFERENT SIMULATED SPEED VARIATIONS. $2\times$, $4\times$, $8\times$, $16\times$ OF ORIGINAL VEHICLE SPEED ARE SIMULATED BY TEMPORALLY DOWNSAMPLING FRAMES, LABELED AS mAP^2 , mAP^4 , mAP^8 , mAP^{16} , RESPECTIVELY. BEST MAP SCORES ARE INDICATED IN BOLD.

Model sizes	Methods	mAP^2	mAP^4	mAP^8	mAP^{16}
S	LongShortNet-S	26.4	20.6	13.4	8.9
	DAMO-StreamNet-S	28.9	22.0	14.6	9.4
	CorrDiff-S(Ours)	29.3	22.5	15.1	10.0
	CorrDiff-S*(Ours)	29.1	23.1	16.2	12.1
M	LongShortNet-M	30.7	23.8	15.8	9.7
	DAMO-StreamNet-M	31.7	24.4	16.0	10.2
	CorrDiff-M(Ours)	32.1	24.9	16.6	11.1
	CorrDiff-M*(Ours)	31.9	25.4	17.2	12.8
L	LongShortNet-L	33.2	25.8	17.2	10.7
	DAMO-StreamNet-L	33.8	26.1	17.1	10.8
	CorrDiff-L(Ours)	34.5	26.9	17.6	11.1
	CorrDiff-L*(Ours)	33.8	27.5	19.6	14.2

(large). These configurations differ in the number of model parameters. The configuration setting is in accordance with previous methods' approaches [10], [14].

Main Metric: We follow the streaming evaluation methods proposed by [15] as the main test metric. The streaming Average Precision (sAP) is used to evaluate the performance of the whole pipeline under a simulated real-time situation. The sAP metric compares the output of the model with ground-truth at output timestamp, instead of input timestamp, which is common in offline evaluations. Specifically, the sAP metric realigns the prediction at time t_i^{out} to index j in order to match the indices of ground truth. Each index $j \in [0, L)$ is paired with the nearest prediction before the emission of frame I_j . In other words, each ground truth item in $\{O_j\}$ is paired with an item in detector output $\{\hat{O}_i\}$, while satisfying

$$t_i^{out} \leq t_j^{in}, t_j^{in} < t_{i+1}^{out}. \quad (7)$$

Note that it is possible that some consecutive ground truth frames are assigned to the same prediction frame, due to the fact that the delay costs more time than the frame time (33ms, typically). The prediction and ground-truth pairs are then evaluated via common detection metrics, such as mean Average Precision (mAP), which computes the average precision scores of matched objects with IoU thresholds ranging from 0.5 to 0.95. The sAP scores for small, medium, and large objects (denoted as sAP_S , sAP_M , sAP_L respectively) are also reported. To ensure a fair comparison, we did not employ mixed speed training under the main metric. This is in accordance with the training scheme of baseline methods.

TABLE IV
THE HARDWARE SPECIFICATIONS OF FOUR DEVICES USED IN THE EXPERIMENT.

Device Name	CPU	GPU	Memory
2080Ti server	Intel(R) Xeon(R) Gold 5118 CPU @ 2.30GHz × 48	NVIDIA GeForce RTX 2080 Ti × 4	257547MB
3090 server	Intel(R) Core(TM) i9-10980XE CPU @ 3.00GHz × 36	NVIDIA GeForce RTX 3090 × 2	128527MB
4080 server	Intel(R) Core(TM) i9-10900X CPU @ 3.70GHz × 20	NVIDIA GeForce RTX 4080 × 2	257420MB
v100 cluster	Intel(R) Xeon(R) Gold 6226 CPU @ 2.70GHz × 24	Tesla V100-SXM2-32GB × 8	256235MB

TABLE V

ABLATION STUDY ON DESIGN VARIATIONS OF CORRDIFF-S. ALL THE FOUR COMPONENTS PRESENTED IN THIS TABLE ARE HELPFUL IN OUR FRAMEWORK. SINCE PLANNER AND BUFFER ONLY FUNCTION UNDER STREAMING TESTS, WE SPLIT THE ABLATION STUDY INTO TWO PARTS EVALUATED BY mAP AND sAP, RESPECTIVELY. WE ALSO INVESTIGATE DIFFERENT VARIATIONS OF THE CORR_PAST AND DIFF_NOW MODULES. NOTE THAT THE BUFFER MODULE IS CRUCIAL IN STREAMING PERCEPTION SETTINGS BY AVOIDING HUGE COMPUTATION COST, BOTH FOR CORRDIFF AND BASELINE METHODS. BEST SCORES ARE INDICATED IN BOLD.

Corr_Past	Diff_Now	mAP	mAP ₅₀	mAP ₇₅
×	×	29.0	50.1	29.1
×	concatenate	30.8	51.9	30.6
×	addition	31.2	52.3	31.1
×	✓	31.5	52.6	31.5
channel-wise	✓	31.8	52.9	31.7
✓	✓	32.2	53.2	32.1
Planner	Buffer	sAP	sAP ₅₀	sAP ₇₅
×	×	3.9	5.8	4.1
×	✓	31.6	52.7	31.5
✓	✓	32.1	53.2	32.1

Delay Adaptation Metric: To simulate streaming perception on devices with diverse connectivity and computation capabilities, we test the framework on 1 online GPU computing cluster (denoted as v100 cluster) and 3 real-world servers (denoted as 4080 server, 3090 server and 2080Ti server) with different hardware specifications. The detailed information about these devices is listed in Table IV. Additionally, we adopt a delay factor d to simulate various delay situations, where all communication-computational delays are multiplied by d . We assign $d \in \{2, 4, 8, 16\}$ and denote corresponding sAP value as sAP^d .

Acceleration Adaptation Metric: To offer a more comprehensive comparison, we also evaluate the models (w/o strategy algorithm) under an offline setting using mean Average Precision (mAP). This approach ignores the impact of communication and computational delay, only simulates different amplitudes of vehicle acceleration by temporally downsampling frames. This metric tests the model’s ability to handle various object displacements between adjacent frames. Unlike common offline evaluations, the prediction \hat{O}_i is evaluated against future objects $\{O_{i+d}\}$, $d \in \{2, 4, 8, 16\}$. The resulting mAP scores are denoted as mAP^2 , mAP^4 , mAP^8 , mAP^{16} , respectively.

B. Quantitative Results

Overall Performance Comparison: As the main result, our framework is evaluated against SOTA methods to demonstrate its strengths. Our proposed method achieves 38.1% in sAP, as shown in Table I, surpassing the current SOTA method by 0.3%. Under S and M configurations, our pipeline also achieves

TABLE VI

ABLATION STUDY ON DIFFERENT TRAINING SPEED OF CORRDIFF-S. $1\times, 2\times, 4\times, 8\times$ DENOTES TRAINING WITH A FIXED SPEED RATE $d \in \{1, 2, 4, 8\}$, RESPECTIVELY. MIXED DENOTES TRAINING WITH RANDOM SPEED RATE d , SAMPLING FROM $\{1, 2, 4, 8\}$ IN EVERY ITERATION. BEST SCORES ARE INDICATED IN BOLD.

Training Speed	sAP ¹	sAP ²	sAP ⁴	sAP ⁸
1x	32.1	30.1	24.7	17.6
2x	28.1	26.1	22.5	15.7
4x	18.4	16.5	14.4	11.3
8x	12.6	10.1	9.4	7.9
Mixed	31.6	30.3	25.0	17.9

the first place in most metrics, compared to [25], [14] and [10]. The results clearly demonstrate the power of CorrDiff. Note that sAP_L of our models is high, indicating that our proposed CorrDiff has recognized the temporal movement of large objects.

sAP Comparison for Delay Adaptation: To demonstrate the robustness of CorrDiff, we employ the Delay Adaptation Metric and evaluate both our framework and baseline models across 4 devices with 4 different delay factor d . As illustrated in Table II, our method surpasses current SOTA DAMO-StreamNet [10] by a maximum of 2.6% sAP on numerous real-world devices, demonstrating its strength on computation-bound environments. Notably, in high-latency scenarios, LongShortNet surpasses DAMO-StreamNet despite using a lighter backbone, indicating that large models do not necessarily scale effectively with increased latency. The result indicates that our method maintains its performance superiority even on devices with poor connectivity or low computing power.

mAP Comparison for Acceleration Adaptation: We also compared our method in simulated situation with drastic object accelerations. We evaluate our framework both with and without mixed speed training, to investigate the displacement adaptivity of the detection model. As shown in Table III, our proposed method achieves an absolute improvement of 0.4%, 1.1%, 1.6%, 2.7% under mAP^2 , mAP^4 , mAP^8 and mAP^{16} , respectively, without mixed speed training compared to DAMO-StreamNet-S. Interestingly, although mixed-speed-trained models only have similar performance to other baseline models under mAP^2 , a maximum of 3.4% mAP gain is observed on larger temporal intervals. The experimental results demonstrate the temporal flexibility of our framework.

Device Hardware Specifications As shown in Table IV, our experiment uses four different devices with variations in their communicational and computational capabilities. The Delay Adaptation Metric experiment is done on all four devices, while other experiments are done on the 4080 server. One thing to mention is that although we used different devices from those used in StreamYOLO [25] and DAMO-StreamNet

[10] (RTX 4080 vs Tesla V100), it does not affect the validity of our experiments. Generally, the V100 has similar or even slightly higher deep learning capacity (112 TFlops for V100 vs. 97.42 TFlops for 4080), so we believe the comparison to the SOTAs does not overestimate our method. Additionally, we also evaluated our S model on the V100, which achieved an sAP of 32.1, the same as our 4080 results, further validating the fairness of the comparison.

C. Ablation study

Design Variations: The results of the ablation study are listed in Table V. We verify the effectiveness of four proposed components: Corr_Past, Diff_Now, Planner and Buffers (Historical Feature Buffer, Corr_Diff Buffer and Output Buffer). For Corr_Past and Diff_Now, we remove them from our model and observe a 0.7% and 2.5% decrease in test sAP, respectively. We also test other variations of Corr_Past and Diff_Now. For Corr_Past, we tested other correlations such as per-channel correlation. For Diff_Now, we tested concatenation or addition operation between the features. However, all substitutions are inferior to our current approach. As for Planner and Buffers which only operate under streaming settings, we examine their ability under sAP. We remove them from our framework and observe a 0.5% and an astonishing 27.7% decrease in the metric. The huge decrease in sAP indicates that it is unrealistic to recompute past frames' feature under streaming perception settings.

Mixed speed Training: We also employ training under different velocities (by temporally downsampling frames) as well as mixed speed training (by sampling input frames from random frame intervals). The results in Figure VI show that fixing training speed will not necessarily increase sAP under simulated high-delay environments. Instead, mixed speed training increases accuracy in large d values by randomly sampling different input frames' indices (C^P), potentially modeling the objects' movement under different velocities.

VI. DISCUSSION

Conclusion: We introduce CorrDiff, a novel streaming perception framework that utilizes temporal cues to produce multiple predictions that aligns with real-world time, effectively producing real-time detection results. CorrDiff is the pioneer framework in streaming perception that make use of temporal cues and multi-frame output. Inspired from optical flow models, we design the detection model that handles input and output with a dynamic temporal range. The scheduling algorithm is also proposed to provide buffer techniques and temporal cues to the detector. Our method not only outperforms current SOTA methods under ordinary streaming perception settings, but also surpasses these methods by a large margin under high/dynamic communication-computational delay & drastic object acceleration environments.

Limitation: Despite the demonstrated strengths, CorrDiff still has its limitations. First, though temporal cues C^P and C^F are produced to provide runtime information, the detection model only utilizes it in the computation of Corr as a coefficient. A stronger integration could be achieved if it further impacts the computation of features. Second, our Delay Adaptation Metric will sometimes not reflect the true ability of the model due to temporal aliasing effect. In other words, the model will perform poorly if computational time slightly misaligns with multiples of frame rate. For example, if the model's total delay time is slightly over one frame interval (say, 34 ms), at time i , its prediction will be evaluated with ground truth O_{i+2} . If the delay time is 32 ms, its prediction will instead be compared with O_{i+1} , making a large difference from a slight delay change. Therefore, we should sample more values of d (decimal values, instead of integers) to concretely evaluate the model. Third, although we considered the fluctuation of the model's computation time, the evaluation of impacts from different external workloads is not included in our experiment. The reason is that the evaluation may not be deterministic, since the model and the workload could affect each other. E.g., the model could cause the workload's GPU operations to queue, reducing the workload's impact on the model. This interference could introduce uncertainty that makes the results unreproducible. We leave these limitations for future work.

REFERENCES

- [1] Ting-Wu Chin, Ruizhou Ding, and Diana Marculescu. Adascale: Towards real-time video object detection using adaptive scaling. *arXiv preprint arXiv:1902.02910*, 2019.
- [2] Jiajun Deng, Yingwei Pan, Ting Yao, Wengang Zhou, Houqiang Li, and Tao Mei. Relation distillation networks for video object detection. In *Proceedings of the IEEE/CVF International Conference on Computer Vision (ICCV)*, October 2019.
- [3] Christoph Feichtenhofer, Axel Pinz, and Andrew Zisserman. Detect to track and track to detect. In *Proceedings of the IEEE International Conference on Computer Vision (ICCV)*, Oct 2017.
- [4] Zheng Ge, Songtao Liu, Feng Wang, Zeming Li, and Jian Sun. Yolox: Exceeding yolo series in 2021. *arXiv preprint arXiv:2107.08430*, 2021.
- [5] Anurag Ghosh, Vaibhav Balloli, Akshay Nambi, Aditya Singh, and Tanuja Ganu. Chanakya: learning runtime decisions for adaptive real-time perception. *Advances in Neural Information Processing Systems*, 36, 2024.
- [6] Anurag Ghosh, Akshay Nambi, Aditya Singh, Harish Yvs, and Tanuja Ganu. Adaptive streaming perception using deep reinforcement learning. *arXiv preprint arXiv:2106.05665*, 1(2):7, 2021.
- [7] Ross Girshick. Fast r-cnn. In *2015 IEEE International Conference on Computer Vision (ICCV)*, pages 1440–1448, 2015.
- [8] Ross Girshick, Jeff Donahue, Trevor Darrell, and Jitendra Malik. Rich feature hierarchies for accurate object detection and semantic segmentation, October 2014. arXiv:1311.2524 [cs].
- [9] Mingfei Han, Yali Wang, Xiaojun Chang, and Yu Qiao. Mining inter-video proposal relations for video object detection. In Andrea Vedaldi, Horst Bischof, Thomas Brox, and Jan-Michael Frahm, editors, *Computer Vision – ECCV 2020*, pages 431–446, Cham, 2020. Springer International Publishing.
- [10] Jun-Yan He, Zhi-Qi Cheng, Chenyang Li, Wangmeng Xiang, Binghui Chen, Bin Luo, Yifeng Geng, and Xuansong Xie. Damo-streamnet: Optimizing streaming perception in autonomous driving. *arXiv preprint arXiv:2303.17144*, 2023.
- [11] Yihui Huang and Ningjiang Chen. Mtd: Multi-timestep detector for delayed streaming perception. *arXiv preprint arXiv:2309.06742*, 2023.
- [12] Wonwoo Jo, Kyungshin Lee, Jaewon Baik, Sangsun Lee, Dongho Choi, and Hyunwoo Park. Dade: Delay-adoptive detector for streaming perception. *arXiv preprint arXiv:2212.11558*, 2022.
- [13] Lingtong Kong, Chunhua Shen, and Jie Yang. Fastflownet: A lightweight network for fast optical flow estimation. In *2021 IEEE International Conference on Robotics and Automation (ICRA)*, pages 10310–10316, 2021.
- [14] Chenyang Li, Zhi-Qi Cheng, Jun-Yan He, Pengyu Li, Bin Luo, Hanyuan Chen, Yifeng Geng, Jin-Peng Lan, and Xuansong Xie. Longshortnet: Exploring temporal and semantic features fusion in streaming perception. In *ICASSP 2023-2023 IEEE International Conference on Acoustics, Speech and Signal Processing (ICASSP)*, pages 1–5. IEEE, 2023.
- [15] Mengtian Li, Yu-Xiong Wang, and Deva Ramanan. Towards streaming perception. In *Computer Vision–ECCV 2020: 16th European Conference, Glasgow, UK, August 23–28, 2020, Proceedings, Part II 16*, pages 473–488. Springer, 2020.
- [16] Wei Liu, Dragomir Anguelov, Dumitru Erhan, Christian Szegedy, Scott Reed, Cheng-Yang Fu, and Alexander Berg. Ssd: Single shot multibox detector. In *European Conference on Computer Vision*, volume 9905, pages 21–37, 10 2016.
- [17] Ze Liu, Yutong Lin, Yue Cao, Han Hu, Yixuan Wei, Zheng Zhang, Stephen Lin, and Baining Guo. Swin transformer: Hierarchical vision transformer using shifted windows. In *Proceedings of the IEEE/CVF international conference on computer vision*, pages 10012–10022, 2021.
- [18] Niki Parmar, Ashish Vaswani, Jakob Uszkoreit, Lukasz Kaiser, Noam Shazeer, Alexander Ku, and Dustin Tran. Image Transformer, June 2018. arXiv:1802.05751 [cs].
- [19] Joseph Redmon, Santosh Divvala, Ross Girshick, and Ali Farhadi. You only look once: Unified, real-time object detection. In *2016 IEEE Conference on Computer Vision and Pattern Recognition (CVPR)*, pages 779–788, 2016.
- [20] Shaoqing Ren, Kaiming He, Ross Girshick, and Jian Sun. Faster R-CNN: Towards Real-Time Object Detection with Region Proposal Networks. In *Advances in Neural Information Processing Systems*, volume 28. Curran Associates, Inc., 2015.
- [21] Mykhailo Shvets, Wei Liu, and Alexander C. Berg. Leveraging long-range temporal relationships between proposals for video object detection. In *Proceedings of the IEEE/CVF International Conference on Computer Vision (ICCV)*, October 2019.
- [22] Shiyao Wang, Yucong Zhou, Junjie Yan, and Zhidong Deng. Fully motion-aware network for video object detection. In *Proceedings of the European Conference on Computer Vision (ECCV)*, September 2018.
- [23] Haiping Wu, Yuntao Chen, Naiyan Wang, and Zhaoxiang Zhang. Sequence level semantics aggregation for video object detection. In *Proceedings of the IEEE/CVF International Conference on Computer Vision (ICCV)*, October 2019.
- [24] Ran Xu, Chen-lin Zhang, Pengcheng Wang, Jayoung Lee, Subrata Mitra, Somali Chaterji, Yin Li, and Saurabh Bagchi. Approxdet: content and contention-aware approximate object detection for mobiles. In *Proceedings of the 18th Conference on Embedded Networked Sensor Systems*, pages 449–462, 2020.
- [25] Jinrong Yang, Songtao Liu, Zeming Li, Xiaoping Li, and Jian Sun. Real-time object detection for streaming perception. In *Proceedings of the IEEE/CVF conference on computer vision and pattern recognition*, pages 5385–5395, 2022.
- [26] Xizhou Zhu, Jifeng Dai, Lu Yuan, and Yichen Wei. Towards high performance video object detection. In *Proceedings of the IEEE Conference on Computer Vision and Pattern Recognition (CVPR)*, June 2018.
- [27] Xizhou Zhu, Yujie Wang, Jifeng Dai, Lu Yuan, and Yichen Wei. Flow-guided feature aggregation for video object detection. In *Proceedings of the IEEE International Conference on Computer Vision (ICCV)*, Oct 2017.
- [28] Xizhou Zhu, Yuwen Xiong, Jifeng Dai, Lu Yuan, and Yichen Wei. Deep feature flow for video recognition. In *Proceedings of the IEEE Conference on Computer Vision and Pattern Recognition (CVPR)*, July 2017.